

# Flaring Activity of Sgr A\* at 43 and 22 GHz: Evidence for Expanding Hot Plasma

F. Yusef-Zadeh<sup>1</sup>, D. Roberts<sup>2</sup>, M. Wardle<sup>3</sup>, C. O. Heinke<sup>4</sup> and G. C. Bower<sup>5</sup>

## ABSTRACT

We have carried out Very Large Array (VLA) continuum observations to study the variability of Sgr A\* at 43 GHz ( $\lambda=7\text{mm}$ ) and 22 GHz ( $\lambda=13\text{mm}$ ). A low level of flare activity has been detected with a duration of  $\sim 2$  hours at these frequencies, showing the peak flare emission at 43 GHz leading the 22 GHz peak flare by  $\sim 20$  to 40 minutes. The overall characteristics of the flare emission are interpreted in terms of the plasmon model of Van der Laan (1966) by considering the ejection and adiabatically expansion of a uniform, spherical plasma blob due to flare activity. The observed peak of the flare emission with a spectral index  $\nu^{-\alpha}$  of  $\alpha=1.6$  is consistent with the prediction that the peak emission shifts toward lower frequencies in an adiabatically-expanding self-absorbed source. We present the expected synchrotron light curves for an expanding blob as well as the peak frequency emission as a function of the energy spectral index constrained by the available flaring measurements in near-IR, sub-millimeter, millimeter and radio wavelengths. We note that the blob model is consistent with the available measurements, however, we can not rule out the jet of Sgr A\*. If expanding material leaves the gravitational potential of Sgr A\*, the total mass-loss rate of nonthermal and thermal particles is estimated to be  $\leq 2 \times 10^{-8} M_{\odot} \text{yr}^{-1}$ . We discuss the implication of the mass-loss rate since this value matches closely with the estimated accretion rate based on polarization measurements.

*Subject headings:* Galaxies: nuclei — Galaxies: The Galaxy — Radio sources: interferometry

---

<sup>1</sup>Department of Physics and Astronomy, Northwestern University, Evanston, IL 60208 (zadeh@northwestern.edu)

<sup>2</sup>Adler Planetarium and Astronomy Museum, 1300 South Lake Shore Drive, Chicago, IL 60605 (doug-roberts@northwestern.edu)

<sup>3</sup>Department of Physics, Macquarie University, Sydney NSW 2109, Australia (wardle@physics.mq.edu.au)

<sup>4</sup>Department of Physics and Astronomy, Northwestern University, Evanston, IL 60208 (cheinke@northwestern.edu)

<sup>5</sup>Radio Astronomy Lab, 601 Campbell Hall, University of California, Berkeley, CA 94720

## 1. Introduction

There is now compelling evidence that the compact nonthermal radio source Sgr A\* is identified with a massive black hole at the center of the Galaxy. Stellar orbit measurements have shown a mass  $3\text{--}4 \times 10^6 M_\odot$  coincident within 45 AU of Sgr A\*, and have created a much better picture of this object since its discovery more than 30 years ago (Balick & Brown 1974; Schödel et al. 2002; Ghez et al. 2004). The luminosity is thought to be due to accreting thermal winds from its neighboring cluster of massive stars (e.g., Melia 1992). One of the key questions that has attracted much attention recently is why Sgr A\* is so dim. The luminosity of Sgr A\* in each wavelength band is known to be about eight orders of magnitudes lower than the Eddington luminosity, prompting a number of theoretical models to explain its faint emission (e.g., Melia & Falcke 2001; Yuan, Quataert & Narayan 2003; Goldston, Quataert & Tgumenshchev 2005; Liu & Melia 2001; Liu, Melia & Petrosian 2006). Theoretical models for Sgr A\*'s spectrum require a very low efficiency for production of X-rays, considering the substantial mass inflow predicted from gas at the Galactic center. Sgr A\*'s multi-wavelength spectrum was fairly successfully modeled as a two-temperature radiatively inefficient flow which is advected across the event horizon before surrendering its luminosity—an ADAF (Narayan et al. 1998). More recently, detection of radio and sub-millimeter polarization from Sgr A\* (Bower et al. 2003; Marrone et al. 2006) has allowed estimates of the integrated electron density in the accretion region from  $\sim 10$  to 1000 Schwarzschild radii. These estimates indicate much lower electron densities than that predicted by the ADAF model, implying that most of the material is not reaching the central black hole. Theoretical work (e.g., Yuan et al. 2003) supports this picture, but leaves unanswered the question of whether infalling material finds itself in a convective flow (Narayan et al. 2002), a (magnetically-driven) low-velocity outflow (Blandford & Begelman 1999, Igumenshchev et al. 2003), or a fast jet (Yuan, Markoff & Falcke 2002). By studying the flare emission from Sgr A\*, we can potentially address these issues.

Recent multi-wavelength observations of Sgr A\* show that near-IR flare activity is central to the activity in X-ray and sub-mm wavelengths (e.g., Eckart et al. 2004, 2006; Gillessen et al. 2006; Yusef-Zadeh et al. 2006). In particular, the near-IR synchrotron emission is produced by a transient population of  $\sim \text{GeV}$  electrons in a  $\sim 10$  G magnetic field of size  $\sim 10R_s$ . Based on the measurements of the duration of flares that have been detected at near-IR and sub-millimeter wavelengths, arguments have been made that cooling could be due to adiabatic expansion, with the implication that flare activity might be associated with an outflow (Yusef-Zadeh et al. 2006). This interpretation stems from the fact that the

synchrotron lifetime of particles producing  $850\mu\text{m}$  emission is about 12 hours, which is much longer than the 20 to 40-min time scale for the GeV particles responsible for the near-IR emission. In order to test the expanding model of flares, we carried out simultaneous radio continuum observations at 43 and 22 GHz to search for a time delay in the peak frequency emission. The measurements presented here concentrate on the short term variability of Sgr A\* whereas previous measurements at centimeter wavelengths have been concerned with the long term variability of Sgr A\* (Zhao et al. 2003; Herrnstein et al. 2004). Recent study of the long term variability of Sgr A\* at these wavelengths suggests that interstellar scattering is likely to be responsible for the flux density variation of Sgr A\* (Macquart & Bower 2005). Another important aspect of the present observations is that multiple frequency observations of Sgr A\* have been carried out simultaneously for the first time using the fast-switching technique at high frequencies,

Here, we report a weak flare that lasts for about two hours at 43 GHz ( $\lambda=7\text{mm}$ ) and 22 GHz ( $\lambda=13\text{mm}$ ). The cross-correlation plot of the radio data shows a time delay which is accounted for in terms of a phenomenological model of a uniformly expanding plasma blob from Sgr A\*.

## 2. Observations and Data Reductions

We used the Very Large Array (VLA) of the National Radio Astronomy Observatory<sup>6</sup> to observe Sgr A\* simultaneously at 43 and 22 GHz in the BnA array configuration on Feb. 10 and 11, 2005 for 4 hours each. The second day of the observing was washed out due to rain. The fast switching mode was used to quickly alternate between Sgr A\* (4 minute) and a nearby ( $8.6'$  from Sgr A\*) source 1820-254 (1 minute) at each frequency. This allowed us to apply a complex gain calibration determined for the calibrators frequently throughout the run. The calibration of the phases were done at high temporal resolution (every 10 seconds). 3C286 was used as a primary gain calibrator and NRAO 530 was observed every 15-30 minutes as a calibration check and in order to calibrate 1820-254. The gains determined for the calibrators were applied to Sgr A\*, which was subsequently phase self-calibrated using the bright ( $\sim 2$  Jy) point source itself for visibility spaces beyond  $100$  kilo $\lambda$ . An additional phase self-calibration was applied using the best clean component model, following a point-source self-calibration on Sgr A\*. This allowed us to calibrate the phases for baselines longer than  $20$  kilo $\lambda$ . In order to compare the variability of Sgr A\* against that of a calibrator, we

---

<sup>6</sup>The National Radio Astronomy Observatory is a facility of the National Science Foundation, operated under a cooperative agreement by Associated Universities, Inc.

applied the derived complex gains from NRAO 530 to 1820-254 and carried out an additional point-source phase self-calibration.

In order to examine if there is a time delay in the light curve of Sgr A\* between 43 and 22 GHz data, we used the z-transformed discrete correlation function (ZDCF) (Alexander, 1997). The ZDCF is an improved solution to the problem of investigating correlation in unevenly sampled light curves. The standard solutions are interpolation of the existing light curve, which is considered to be unreliable when power exists on smaller time scales than the gaps, and binning the data using discrete correlation functions (DCFs) (e.g. Edelson & Krolik 1988). In DCFs, all pairs of points are ordered according to their time differences, binned, and compared. The ZDCF improves upon standard DCFs by the application of the z-transform, which brings the skewed distribution of the DCF closer to a normal distribution. The ZDCF chooses the binning of the data points to give equal populations in each bin, with a requirement that there be  $>11$  points in each bin.

### 3. Results

The light curves corresponding to 43 and 22 GHz data for Sgr A\* and the nearby calibrator 1820-254 are shown in the top panels of Figures 1 and 2, respectively. The fluxes presented in the light curves were derived by fitting a point source at the phase center in the visibility plane using spacings beyond 100 kilo- $\lambda$ . The measurements of the fluxes from this technique were taken every 60 seconds. The light curve of Sgr A\* shows an increase of flux at a level of 7% and 4.5% at 43 and 22 GHz, respectively, when compared to its quiescent flux, whereas the flux of the calibrator remains constant. For Sgr A\*, the rise and fall time scale of 1.5 – 2 hours noted in these measurements is similar to the flare time scale seen in sub-millimeter as well as millimeter wavelengths (Yusef-Zadeh et al. 2006; Mauerhan et al. 2005; Eckart et al. 2006). The variability analysis of several observations of Sgr A\* at 43 GHz has also shown a 2-4 hour typical time scale (Roberts et al. 2006).

The results of the cross correlation analysis of Sgr A\* and 1820-254 are shown in the bottom panels of Figures 1 and 2, respectively. The cross-correlation peak of Sgr A\*, as shown in Figure 1, is seen at negative lag time, implying that the 22 GHz flare can not be leading the flare emission at 43 GHz. No peak is seen in the cross-correlation plot of 1820-254 whereas Sgr A\* shows the appearance of two peaks with a delay of  $\sim 20$  and 50 minutes between 43 and 22 GHz for Sgr A\*. Due to the fact that the cross-correlation peaks are broad, we can not rule out the possibility of zero time delay. However, we believe it is unlikely, given that both peaks are clearly not centered at zero time delay.

The spectral index measurements of the flaring and the quiescent phase of Sgr A\* have also been made. We begin by subtracting a constant flux density of  $S_\nu = 1.63$  and  $1.11$  Jy from the combined flux density of the quiescent and flare emission at 43 and 22 GHz, respectively. The average spectral index ( $S_\nu \propto \nu^\alpha$ ) of the flare is estimated to be  $\alpha = 1.18 \pm 0.017$ , which is steeper by a factor of two than that of the quiescent emission, ( $0.58 \pm 0.004$ ). The spectral index of the peak emission is 1.56 assuming a maximum flux density of the flare  $S_\nu^m = 148$  and  $52$  mJy at 43 and 22 GHz, respectively. Since the measurements of the light curves of the flare at 43 and 22 GHz are interleaved throughout the observing period, there is some uncertainty as to the exact value of the peak flux density at 43 GHz, considering that there is no data around the time of the peak flux. Additional uncertainty in determining the spectral index of the flare emission comes from a simple average of the parts of the light curve that was taken on either side of the flare. Since the flare started near the beginning of the run and the fact that the quiescent emission appears to have structure (i.e., not completely constant), a simple average is unlikely to be correct. It is difficult to quantify the uncertainty which could affect the peak flux of the flare emission. This is the first time that such a flare emission has been seen simultaneously at 22 and 43 GHz using the fast-switching technique. We hope that future high-resolution VLA observations address the true quiescent flux of Sgr A\* at these high radio frequencies. Recent 43 GHz measurements of Sgr A\* show a great deal of variability in the so-called quiescent flux of Sgr A\* (Roberts et al. 2006).

Given the uncertainties described above, we measured the variation of the spectral index as a function of time which shows a steep spectral index of  $\alpha \sim 2.4$  at the beginning of the flare before it flattens out towards the end of the flare. The steep value of  $\alpha$  at the beginning of the flare is due to the fact that the peak of emission at 43 GHz leads that at 22 GHz. It is instructive to note that snapshot observations at radio wavelengths could give a misleading spectral index distribution when there is a time delay between the peak emission at different frequencies.

## 4. Discussion

### 4.1. The Plasmon Model

The near-IR flaring of Sgr A\* is generally thought to be due to optically-thin synchrotron emission from a transient population of particles produced within  $\sim 10$  Schwarzschild radii of the massive black hole (e.g., Genzel et al. 2003; Eckart et al. 2006; Gillessen et al. 2006; Yusef-Zadeh et al. 2006). We have argued recently (Yusef-Zadeh et al. 2006) that the sub-millimeter flare observed simultaneously with a near-IR flare implies that the emission is also optically thin at 350 GHz ( $\lambda=857\mu\text{m}$ ). The  $\sim 30$  minute duration of the flares at both

frequencies strongly suggests that the decline is not due to synchrotron cooling (estimated to be  $\sim 20$  minutes and  $\sim 12$  hours at 1.6 (188 THz) and 850 (350 GHz)  $\mu\text{m}$  respectively) but due to adiabatic cooling associated with expansion of the emitting plasma.

The time delay we have observed between flaring at 43 and 22 GHz is consistent with this picture: as the synchrotron optical depth  $\propto \nu^{-2.5}$ , the emission at these frequencies is initially optically thick. The intensity grows as the blob expands, then peaks and declines at each frequency once the blob becomes optically thin. This first occurs at 43 GHz, and then at 23 GHz about 30–60 minutes later.

To consider this quantitatively, we apply the plasmon model of van der Laan (1966). In this model, flaring at a given frequency is produced through the adiabatic expansion of an initially optically-thick blob of synchrotron-emitting relativistic electrons. The initial rise of the flux is produced by the increase in the blob’s surface area while it still remains optically thick; the curve turns over once the blob becomes optically thin because of the reduction in magnetic field, the adiabatic cooling of the electrons, and the reduced column density as the blob expands. The magnetic and the particle energy density both drop as  $R(t)^{-4}$  where  $R$  is the increasing radius of the plasmon. The model predicts simultaneous flaring and declining emission at high frequencies, which are optically thin, and increasingly delayed flaring at successively lower frequencies that are initially optically thick.

Following van der Laan (1966), the synchrotron flux from a homogeneous blob can be written as

$$S_\nu(R) = S_0 \left( \frac{\nu}{\nu_0} \right)^{2.5} \left( \frac{R}{R_0} \right)^3 \frac{1 - \exp(-\tau)}{1 - \exp(-\tau_0)} \quad (1)$$

where  $R(t)$  is its radius,  $p$  is the index of the relativistic particle energy spectrum ( $n(E) \propto E^{-p}$ ), and the optical depth

$$\tau = \tau_0 \left( \frac{\nu}{\nu_0} \right)^{-(p+4)/2} \left( \frac{R}{R_0} \right)^{-(2p+3)} \quad (2)$$

Here  $\tau_0$  is the critical optical depth at the maximum of the light curve at any frequency, which satisfies

$$e^{\tau_0} - (2p/3 + 1)\tau_0 - 1 = 0 \quad (3)$$

and  $\nu_0$  is the frequency at which this occurs when  $R = R_0$ . The equivalent expression to (3) in van der Laan (1966) has a different coefficient of  $\tau_0$  because his expression is for the optical depth corresponding to the maximum in the spectrum at some instant ( $\partial_\nu S(\nu, t) = 0$ ) rather than the maximum in the light curve at a particular frequency ( $\partial_t S(\nu, t) = 0$ ). To obtain numerical values, we assume that a typical near-IR flare with flux 1 mJy at 1.6  $\mu\text{m}$  (Yusef-Zadeh et al. 2006) is produced by a population of relativistic electrons between 10 MeV

and 3 GeV in equipartition with the magnetic field. The population is confined to a blob characterized by initial size  $2R_0$  and an optical depth that yields 1 mJy at  $1.6\mu\text{m}$ .

The remaining parameters in this model are the spectral index of particles ( $p$ ) and the initial blob radius ( $R_0$ ). We first show the light curves (Fig. 3) at 350, 96, 43 and 22 GHz for the choices  $p = 3$  and  $R_0 = 3R_s$  (for a  $3.7 \times 10^6 M_\odot$  black hole), which give a reasonable match to our 43 and 22 GHz data. For this choice of  $p$ , the critical optical depth is  $\tau_0 = 1.9$  and the corresponding peak frequency is initially  $\nu_0 \approx 130$  GHz ( $\lambda=2.3\text{mm}$ ). The horizontal axis shows the expansion factor over the original blob size; a form of  $R(t)$  must be adopted to map this to time, here we simply assume that  $R \propto t$ . The blob is initially optically thin above 130 GHz, and so the 350 GHz flux declines monotonically as the blob expands. This is consistent with our recent multi-wavelength observing campaign in which apparently simultaneous flares were detected at  $850 \mu\text{m}$  and  $1.6\mu\text{m}$ , although we can not rule out the possibility that the sub-mm flare was delayed by about 100 minutes with respect to an earlier near-IR flare (Yusef-Zadeh et al. 2006). The peak at 96 GHz ( $\lambda=3\text{mm}$ ) is attained rather quickly, as its initial optical depth is  $\approx 6$  and drops as  $R^{-9}$ . The amplitudes of the flares at 96 and 350 GHz are consistent with the intensity fluctuations observed at these frequencies (Miyazaki, Tsutsumi & Tsuboi 2004; Mauerhan et al. 2005; Marrone et al. 2006); unfortunately simultaneous observations at these frequencies are not available at present. The observed  $\sim 30$  minute delay between the peaks at 22 and 43 GHz sets the time scale for the light curves: the plasmon must double its original size in  $\sim 1$  hour. We expect the 96 GHz flux to have peaked  $\sim 30$  minutes before the 43 GHz flare, and about 10 minutes after the near-IR and sub-millimeter flares.

Now we turn to the dependence on the particle index  $p$ . Equations 1 and 2 imply that the frequency at which the light curve is just peaking is

$$\nu_p = \nu_0 \left( \frac{R}{R_0} \right)^{-(4p+6)/(p+4)}, \quad (4)$$

with peak flux

$$S_p = S_0 \left( \frac{\nu_p}{\nu_0} \right)^{(7p+3)/(4p+6)} = \left( \frac{R}{R_0} \right)^{-(7p+3)/(p+4)}. \quad (5)$$

The ‘‘spectral index’’  $\alpha$  of the peak fluxes ( $S_p \propto \nu_p^\alpha$ ) is only weakly dependent on the particle index  $p$ , ranging from 1.21 to 1.55 as  $p$  runs from 2 to 8.

To illustrate the above point, the peak fluxes attained at 350, 96, 43 and 22 GHz during the subsequent evolution of the  $R_0 = 3R_s$  blob are plotted as a function of the electron power-law index  $p$  in Fig. 4. The horizontal lines indicate nominal peak fluxes at the four frequencies – from our measurements at 22 and 43 GHz, and at 96 GHz and at 350 GHz by

Mauerhan et al. (2005) and by Marrone et al. (2006), respectively. Note that the nominal 96 and 350 GHz flux measurements have not been carried out simultaneously with those at 43 and 22 GHz. For the two lowest frequencies, the peak flux always corresponds to the transition from optically thick to optically thin. In the mm and sub-mm, the initial blob is not optically thick if  $p \lesssim 2.5$  and  $p \lesssim 3.7$  respectively, and the flux at those frequencies then decays monotonically with time; hence the rapid decline in peak flux at small values of  $p$ .

Several points are apparent from Fig. 4. First, provided that the blob is initially optically thick at the frequencies of interest, there is a slow increase in spectral index of the peak fluxes as  $p$  is increased, as dictated by equation 5. Our observed spectral index of 1.56 formally corresponds to  $p = 8.41$ . While this is consistent with the spectral index range reported in near-IR synchrotron flares (Eisenhower et al. 2005; Gillessen et al. 2006), such a steep particle spectrum overproduces the flux in sub-mm flares by a factor of 5. In fact  $p$  is very sensitive to  $\alpha$  and so is poorly determined by our observations. For example, a 25% increase in the observed flux at 22 GHz would imply  $p \approx 3$ . On the other hand, the ratios of the peak fluxes at the three lower frequencies *are* fixed by this model *and* match the typical values that have been found (although the 96 GHz observations do not strictly correspond to our particular flares). Third, the nominal peak fluxes at the three lower frequencies can be matched for  $p \approx 3$  or  $p \approx 8$ , but the sub-millimeter flux only matches for  $p \approx 3$ , when the initial blob is optically thin. We therefore conclude that  $p \approx 3$  for our nominal fluxes.

The initial blob size  $R_0$  and particle spectral index  $p$  are strongly constrained by the combination of measurements at frequencies that are initially optically thin ( $\nu > \nu_0$ ) and optically thick ( $\nu < \nu_0$ ). The initial flux at frequencies above  $\nu_0$  is tied to the assumed near-IR flux by the particle spectral index and do not depend on the assumed source size. The blob size does affect the peak flux in the light curves of frequencies below  $\nu_0$  by determining the initial optical depth. We have also plotted the peak fluxes obtained for  $R = 5R_s$ . This increases the fluxes at 22, 43, and 96 GHz, and shifting the match to  $p \approx 2.5$  and reducing the 350 GHz flux to  $\sim 100$  mJy.

The plasmon model, while phenomenological, is surprisingly instructive. It's clear that simultaneous monitoring of Sgr A\* at several frequencies between 10 and 100 GHz to determine the peak fluxes and time delays will be able to test the model's applicability. Adding simultaneous monitoring at two frequencies above  $\sim 200$  GHz, where the initial blob is optically thin, should allow measurement of the flare parameters on a flare-by-flare basis.

Meanwhile, we can make some physical inferences based on the estimates  $p \approx 3$  and  $R \approx 4R_s$ . The observed delay,  $\sim 30$  minutes between 22 and 43 GHz, implies that the plasmon expands at a rate  $R_0/\text{hr}$ , or  $\approx 0.02c$ . The equipartition field strength is  $\approx 22$  G, and the number density of relativistic electrons between 10 MeV and 3 GeV is  $\approx 6 \times 10^5 \text{ cm}^{-3}$ .



Adding an equal number of protons to preserve charge neutrality implies a minimum blob mass  $\sim 4 \times 10^{19}$  g. In the absence of significant external pressure the natural expansion speed is the internal sound or Alfvén speed,  $\sim 0.2c$ . The fact that it expands more slowly implies either that it is confined by external pressure or that its density is a hundred times greater than the estimate above because of the presence of a thermal gas component. The mass of the blob would then be  $\sim 4 \times 10^{21}$  g. If this component is in energy equipartition with the field, its temperature would be  $\sim 1 \times 10^9$  K.

If the near-IR flares occur about once per hour and the blobs escape the system (though this appears highly unlikely given the slow inferred expansion speed) the mass loss rate, including the thermal component, would be  $\sim 2 \times 10^{-8} M_{\odot} \text{ yr}^{-1}$ . This mass-loss rate is roughly similar or less than the mass accretion rate estimated from the integrated electron density in the innermost  $\sim 10$  to 1000 Schwarzschild radii of the accretion disk imposed by the rotation measure measurements (Marrone et al, 2006). The combined accretion and mass-loss rate from Sgr A\* is still less than the Bondi-Hoyle accretion rate of  $\sim 10^{-6} M_{\odot} \text{ yr}^{-1}$  estimated from X-ray measurements (Baganoff et al. 2003). Given the  $0.5''$  spatial resolution of *Chandra*, this suggests that the X-ray measurements of Sgr A\* could be contaminated by thermal X-ray flux from the cluster of massive S stars distributed within  $0.5''$  of Sgr A\*. The spectral properties of this cluster of stars show massive stars but are generally consistent with normal main sequence O8V/B0V to B9V stars (Eisenhauer et al. 2005; Baganoff et al. 2003; Nayashkin & Sunyaev 2005). Early B stars tend to contribute between  $10^{30}$  and  $10^{31}$  ergs  $\text{ s}^{-1}$  per star in the 2-8 keV band (Feigelson et al. (2002). Ten of these early B-type stars combined with potentially X-ray emitting low-mass stars could contribute a substantial portion of the soft diffuse emission, thus lowering the estimate of the Bondi rate. Alternatively, we speculate that the mass-loss rate from the young cluster near Sgr A\* is over-estimated or that the accreting thermal winds from the neighbouring cluster is obstructed as they approach Sgr A\*.

## 4.2. Alternative Models

There is a great deal of recent theoretical studies shedding light on other alternative models to explain the flaring activity of Sgr A\*. The flare emission has also been described by a jet model and an orbiting hot spot model (e.g., Eckart et al. 2006; Broderick & Loeb 2006). However, we believe it is not necessary to discuss these alternative models in detail as there is no evidence that Sgr A\* showing either a jet or a disk. Given that the orbiting hot spot model predicts no time delay in flare emission (see Figure 11 of Broderick and Loeb 2006), we briefly view the expanding blob in the context of a jet model.

It is also possible that the expanding blob is confined by a jet that can account for the overproduction of sub-millimeter flare emission when the particle spectrum is steep. In the context of a jet model, one can consider the decreasing peak frequency in terms of an inhomogeneous jet model in which the magnetic field density and particle energy density decrease as powerlaws in distance with indices  $m$  and  $n$ , respectively (e.g., Konigl 1981). The self-absorption frequency, then, is proportional to  $r^{-k}$ , where  $k = [(2 + p)m + 2n - 2]/(4 + p)$ . We consider two distinct cases, where magnetic and particle energy density losses are alternatively dominant. In both cases, we assume  $p = 3$  and an outflow that originates at 10 Schwarzschild radii with velocity  $v \sim c$ . In the first case, we assume  $m = 1$  and  $n = 0$  and find  $k = 3/7$ . The time for the peak frequency to decrease by a factor of two is  $t_2 \sim 1000$  sec. In the second case, we assume  $m = 0$  and  $n = 2$  and find  $k = 2/7$  and  $t_2 \sim 2000$  sec. These values are similar to the time delay observed between 43 and 22 GHz peak emission. Thus, relativistic outflow in an inhomogeneous jet is another possibility that can account for the observed time delay in radio wavelengths.

Given that the overall characteristics of flare emission from Sgr A\* are similar to those of X-ray binaries and microquasars, the jet model has been successfully applied to a number of sources such as GRS 1915+105 (e.g., Mirabel et al. 1998; Fender & Pooley 1998; Fender & Belloni 2004) and Cyg X-3 where the frequency dependent of the peak flux density is in the optically thick domain due to synchrotron self-absorption or free-free absorption (Marti et al. 1992). The jet model of Sgr A\* has also been explored in other contexts to explain the broad band spectrum of its quiescent flux (e.g., Falcke & Markoff 2000), its near-IR variability (Eckart et al. 2004; 2006), as well as the linear and circular polarization measurements (e.g., Falcke & Beckert 2002).

Additional circumstantial evidence that there may be collimated outflow from Sgr A\* comes from the morphology of ionized gas distributed outside the inner 0.5'' of Sgr A\* (Yusef-Zadeh, Morris & Ekers 1990; Zhao et al. 1991). A chain of blob-like structure was noted best to link to Sgr A\* by a ridge of emission at 8 GHz (Wardle & Yusef-Zadeh 1992). These blobs are estimated to have a mass of  $10^{-2} M_{\odot}$  each with a size of about 0.5 to 1''. Although these blobs were considered to be formed as a result of the focusing of the IRS 16 cluster wind by the gravitational potential of Sgr A\* (Wardle & Yusef-Zadeh 1992), it is possible to consider the ridge of blob-like emission resulting directly from a jet associated with Sgr A\*. Future proper motion measurements of the blobs as well as modeling of flaring jet emission from Sgr A\* should be explored in more detail, in spite of a lack of direct evidence for collimated outflow from Sgr A\*.

## 5. Conclusions

Radio continuum measurements using a fast switching technique between 43 and 22 GHz frequencies show a weak flare with a duration of about two hours and time delay between the peak frequency emission. The adiabatic expansion of a uniform spherical synchrotron-emitting plasma blob based on the model by van der Laan (1966) can explain the overall characteristics of the observed flare emission in multiple wavelengths. In particular, the plasmon model is consistent with the time delay observed between the peak 43 GHz and 22 GHz flare emission, the flux values at optically thin radio frequencies and at higher optically thin frequencies. Future simultaneous measurements at optically thin and thick frequencies should test this model.

## REFERENCES

- Alexander, T. 1997, in *Astronomical Time Series*, ed. D. Maoz, A. Sternberg & E. Leibowitz (Dordrecht:Kluwer), 163
- Balick, A. & Brown, R.L. 1974, *ApJ*, 194, 265
- Baganoff, F.K., Maeda, Y., Morris, M., Bautz, M.W., Brandt, W.N. et al. 2003, *ApJ*, 591, 891
- Blandford, R. D. & Begelman, M. C. 1999, *MNRAS*, 303, L1
- Bower, G.C., Wright, M.C., Heino, F. & Backer, D.C. 2003, *ApJ*, 588, 331
- Broderick, A.E. & Loeb, A. 2006, *MNRAS*, 367, 905
- Eckart, A., Baganoff, F. K., Morris, M., Bautz, M.W., Brandt, W.N. et al. 2004, *A&A*, 427, 1
- Eckart, A., Baganoff, F.K., Schoedel, R., Morris, M., Genzel, R., Bower, G.C. et al. 2006, *A&A*, (in press) (astro-ph/0512440)
- Edelson, R.A. & Krolik, J.H. 1988, *ApJ*, 333, 646
- Eisenhauer, F., Genzel, R., Alexander, T., Abuter, R., Paumard, T., Ott, T., Gilbert, A., Gillessen, S., Horrobin, M., Trippe, S. et al. 2005, *ApJ*, 628, 246
- Beckert, T. & Falcke, H. 2002, *A&A*, 388, 1106
- Broderick, A.E. & Loeb, A. 2006, *MNRAS*, 367, 905
- Falcke, H. & Markoff, S. 2000, *A&A*, 362, 113
- Fender, R. & Belloni, T. 2004, *ARAAS*, 42, 317

- Fender, R.P. & Pooley, G.G. 1998, MNRAS, 300, 573
- Feigelson, E. D., Broos, P., Gaffney, J. A., Garmire, G. Hillenbrand, L. A. et al. 2002, ApJ, 574, 258
- Genzel, R., Schödel, R., Ott, T., Eckart, A., Alexander, T., Lacombe, F., Rouan, D., Aschenbach, B. et al. 2003, Nature, 425, 6961, 934
- Ghez, A. M., Wright, S. A., Matthews, K., Thompson, D., Le Mignant, D., Tanner, A., Hornstein, S. D., Morris, M., Becklin, E. E. & Soifer, B. T. 2004, ApJ, 601, L159
- Ghez, A. M., Hornstein, S.D., Lu, J., Bouchez, A., Le Mignant, D. et al. 2005, ApJ, 635, 1087
- Gillessen, S., Eisenhauer, F., Quataert, E., Genzel, R., Paumard, T., Trippe, Ott, T. et al. 2006, ApJ, in press (astro-ph/0511302)
- Goldston, J., Quataert, E. & Tgumenschchev, I.V. 2005, ApJ, 621, 785
- Herrnstein, R.M., Zhao, J.-H., Bower, G.C. & Goss, W. M. 2004, AJ, 127, 3399
- Igumenshchev, I.V., Narayan, R. & Abramowicz, M. A., 2003, ApJ, 592, 1042
- Königl, A. 1981, ApJ, 243, 700
- Liu, S. & Melia, F. 2001, ApJ, 561, L77
- Liu, S., Melia, F. & Petrosian, V. 2006, ApJ, 636, 798
- Macquart, J.-P. & Bower, G.C., 2006, ApJ, in press
- Marrone, D.P., Moran, J., Zhao, J.-H. & Rao, R. 2006, ApJ, in press (astro-ph/0511653)
- Marti, J., Paredes, J.M. & Estalella, R. 1992, A&A, 258, 309
- Mauerhan, J.C., Morris, M., Walter, F. & Baganoff, F. 2005, ApJ, 623, L25
- Melia, F. 1992, ApJ, 387, L25
- Melia, F., & Falcke, H. 2001, ARAA, 39, 309
- Mirabel, I.F., Dhawan, V., Chaty, S., Rodriguez, L.F., Marti, J., Robinson, C.R. et al. 1998, A&A, 330, L9
- Miyazaki, A., Tsutsumi, T. & Tsuboi, M. 2004, ApJ, 611, L97
- Narayan, R., Mahadevan, R., Grindlay, J.E., Popham, R.G & Gammie, C. 1998, ApJ, 492, 554
- Narayan, R., Quataert, E., Igumenshchev, I. V. & Abramowicz, M. A. 2002, ApJ, 577, 29
- Nayakshin, S. & Sunyaev, R. 2005, MNRAS, 364, L23
- Roberts et al. 2006, in preparation

- Schödel, R., Ott, T., Genzel, R., Hofmann, R., Lehnert, M., Eckart, A., Mouawad, N., Alexander, T., Reid, M. J. & Lenzen R. 2002, *Nature*, 419, 694
- van der Laan, H. 1966, *Nature*, 5054, 1131
- Wardle, M. & Yusef-Zadeh, F. 1992, *Nature*, 357, 308
- Yuan, F., Markoff, S., & Falcke, H. 2002, *A&A*, 854, 383
- Yuan, F., Quataert, E. & Narayan, R. 2003, *ApJ*, 598, 301
- Yusef-Zadeh, M., Morris, M. & Eckers, R. 1992, *Nature*, 348, 45
- Yusef-Zadeh, F., Bushouse, H., Dowell, C. D., Wardle, M., Roberts, D., Heinke, C. O., Bower, G. C. et al. 2006, *ApJ*, in press
- Zhao, J.-H., Goss, W. M., Lo, K. Y. & Ekers, R. D. 1991, *Nature*, 354, 46
- Zhao, J.-H., Young, K.H., Hernstein, R.M. et al. 2003, *ApJ*, 586, L29

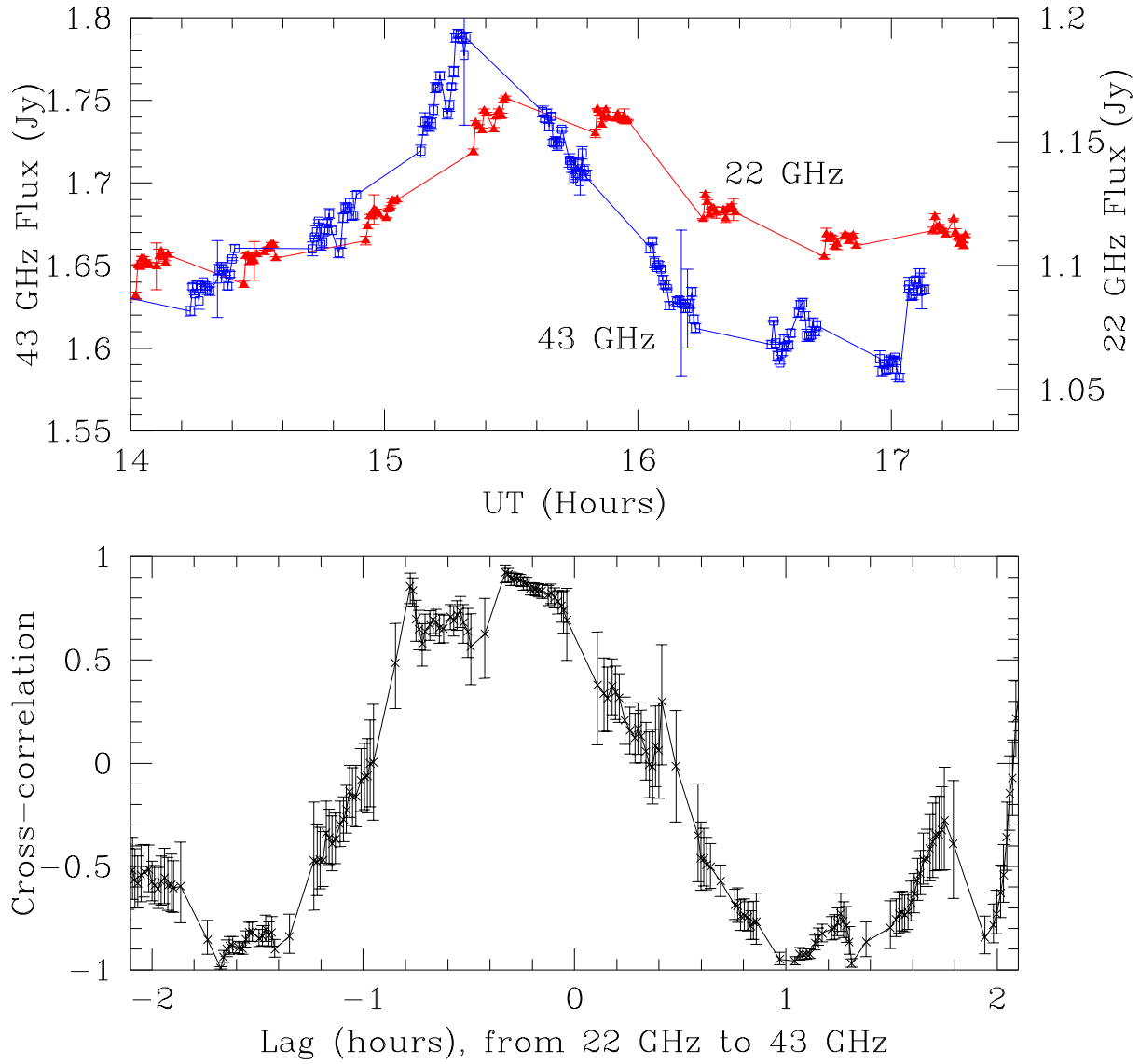


Fig. 1.— (Top) The light curve of Sgr A\* flaring at 43 and 22 GHz with a sampling time of 30 seconds. (Bottom) The cross-correlation amplitude as a function of lag time.

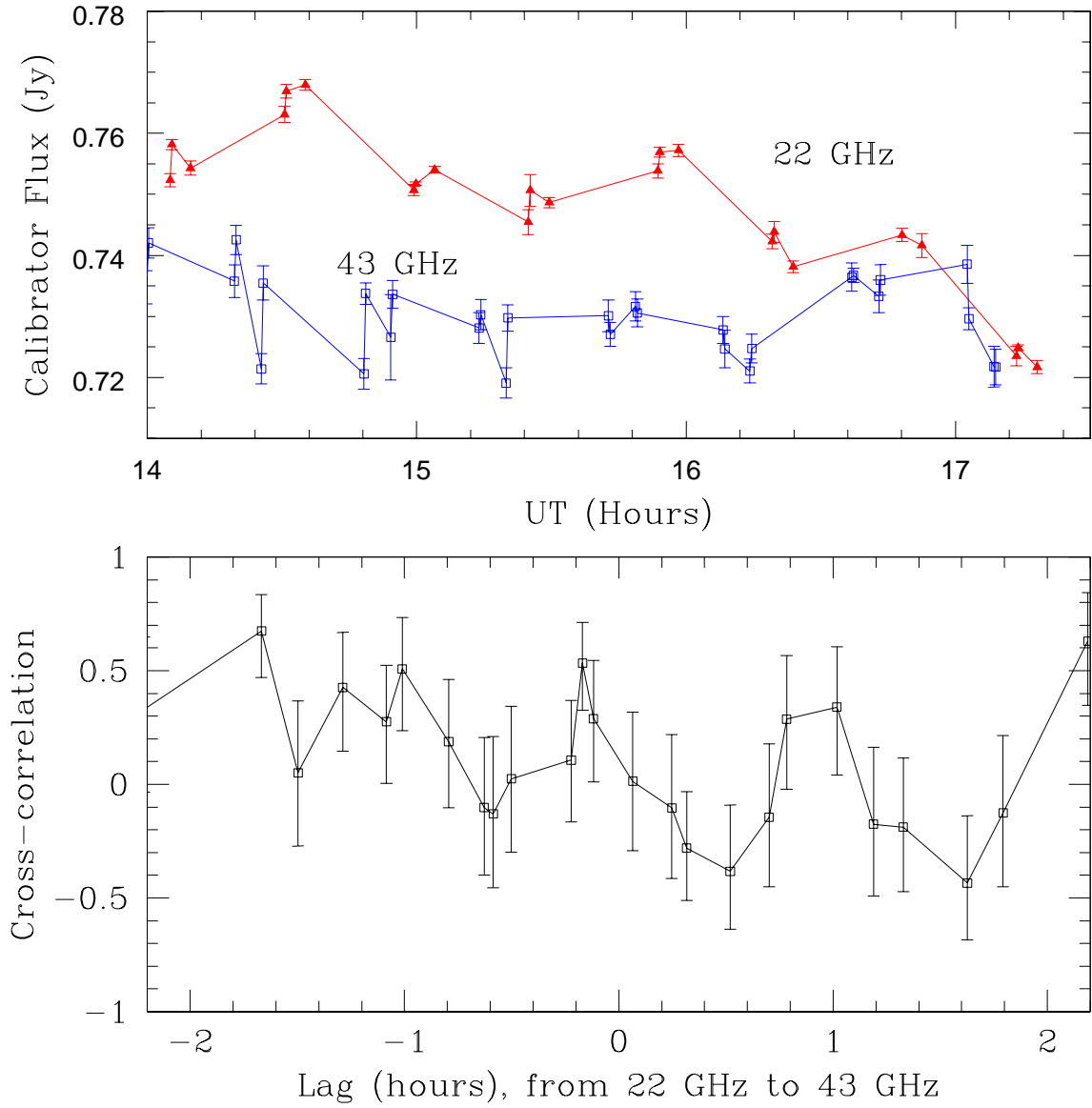


Fig. 2.— (Top) The light curve of 1820-254 showing no variability at 43 (blue) and 22 GHz (red). (Bottom) The cross-correlation amplitude as a function of lag time. The sampling time is 30 seconds.

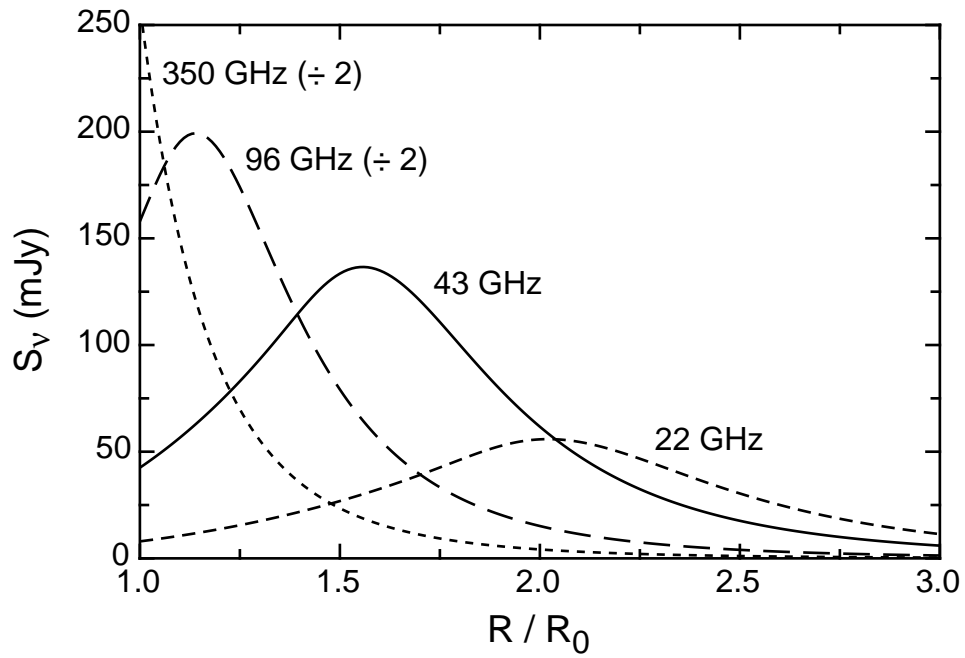


Fig. 3.— Synchrotron light curves at four different frequencies for an expanding blob of plasma with an  $E^{-3}$  electron spectrum in equipartition with its magnetic field. The blob is assumed to have an initial radius  $R_0 = 4R_s$  and near-IR flux of 1 mJy (see text).



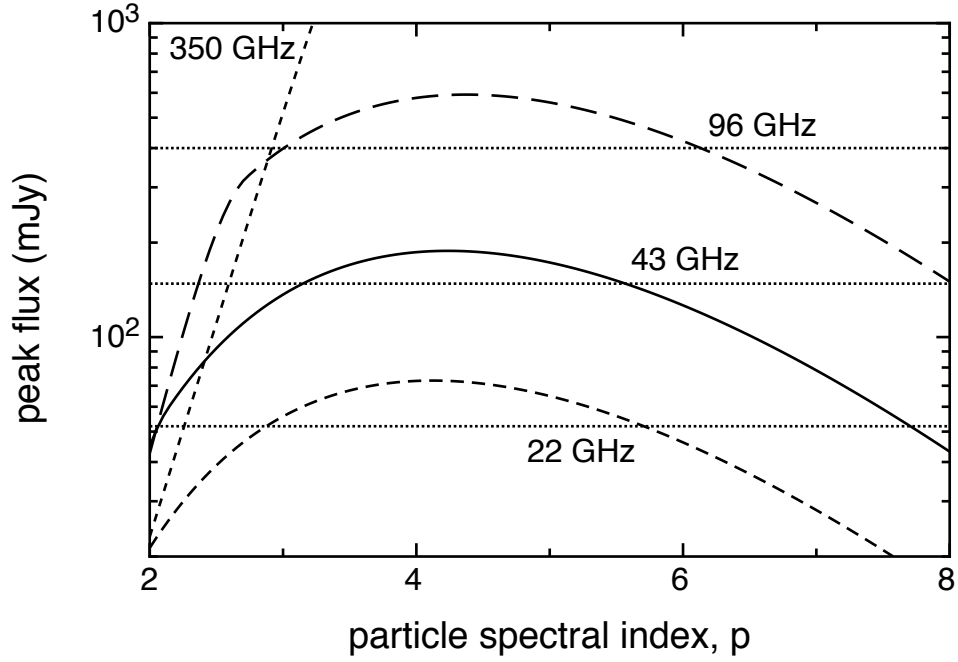


Fig. 4.— Peak flux in the light curves from the blob at four different frequencies as a function of assumed particle spectral index  $n(E) \propto E^{-p}$  (see text). As in Fig. 3, the blob is assumed to have an initial radius  $R_0 = 4R_s$  and near-IR flux of 1 mJy. The dotted horizontal lines indicate the observed peak fluxes of 148, 52 and 400 mJy at 22 and 43 GHz and a typical flare amplitude at 96 GHz (Mauerhan et al. 2005), respectively. The typical flux of a flare at 350 GHz is assumed to be  $\sim 0.5$  Jy. The only simultaneous flux measurements are taken at 43 and 22 GHz.